Prediction of state parameter based on CPT MPM simulations in sandy soils

Mario Martinelli[1,2#] and *Guido* Remmerswaal[1]

[1]*Deltares, Geo-Engineering Unit, Delft 2629 HV, The Netherlands*
[2]*Dept. of Civil and Environmental Engineering, Carleton Univ., 1125 Colonel By Dr., Ottawa, ON, Canada*
[#]*Corresponding author: mario.martinelli@deltares.nl*

ABSTRACT

Cone penetration tests (CPTs) can provide quantitative information about the mechanical state of sandy soils. In the current state of the art, the soil state is derived from the cone resistance, which is estimated from the cavity expansion solution and a calibrated scaling equation. Recently, Martinelli and Pisano (2022) showed that MPM simulations of CPTs provide accurate values of the cone resistance in sandy soils when using the critical state NorSand model. This paper adopts this framework to develop a predictive equation for cone resistance as a function of the NorSand parameters and the state parameter of the soil. This formula is straightforward to implement, and it can be adopted by researchers and practitioners to assess soil state in a soil deposits.

Keywords: CPT, MPM, cone resistance, state parameter.

1. Introduction

A strong correlation exists in sandy soils between the mechanical behaviour and their state, defined by the "state parameter" (ψ) - introduced by Been & Jefferies (1985) - which compares current void ratio with critical state void ratio under the current mean effective stress. In the current state of the art, the state parameter is derived from the cone resistance, which is estimated from the cavity expansion solution and a calibrated scaling equation. Examples can be found in Jefferies and Been (2016) and Ayala et al. (2022).

In recent years, significant progress has been made to accurately simulate CPT data in both sand and clays, using the material point method (MPM) (Ceccato et al. 2016a, 2016b; Martinelli and Galavi, 2021, 2022). More recently, Martinelli and Pisano (2022) demonstrated the predictive capabilities of the critical state NorSand model when used in MPM simulations of CPT to compute cone resistance in sandy soils.

This study adopts the MPM framework proposed by Martinelli and Pisano (2022) with the MPM integration scheme described in Martinelli and Galavi (2022) to simulate CPT chamber tests of loose to medium-dense coarse-grained deposits. These simulations are based on the critical state NorSand model, and they were used to develop a predictive equation for cone resistance. Apart from the soil's state parameter ψ, the other input parameters of the equation are the NorSand parameters, which can be obtained from calibration against triaxial test data of soil samples.

The idea of this paper is to propose a straightforward form of the predictive equation, which can be easily implemented by practitioners to relate - for a specific soil - the cone resistance with the corresponding state parameter ψ, without performing complex and time-consuming large-deformation calculations based on MPM.

2. MPM dataset of cone resistance

This section outlines the key characteristics of the constitutive model and the MPM framework employed for generating synthetic cone resistance data. Additionally, it provides a summary of the parametric study's details.

2.1. MPM model

The MPM code, as outlined by Martinelli & Galavi (2022), adopts a dynamic MPM formulation with soil acceleration used as the primary unknown variable (Jassim et al., 2013). An explicit conditionally-stable time integration scheme is used with automatic adaptation of the time step size. The cone–soil sliding is simulated using the contact algorithm by Bardenhagen et al. (2000). The background mesh is composed of four-node quadrilateral elements with four integration points, and the "moving mesh" concept is adopted to ensure fine discretization around the cone and accurate performance of the contact algorithm (Al Kafaji, 2013). The additional computational aspects are discussed in Martinelli & Galavi (2022).

The sand behavior is modeled using the state-dependent NorSand constitutive model (Jefferies, 1993). The formulation adopts a log-linear critical state line, as follows:

$$e_{cs} = \Gamma_1 - \lambda_e ln(p) \quad (1)$$

where Γ_1 is the void ratio when p is 1 kPa, and λ_e is the slope. The linear elastic shear modulus (G) is expressed by the equation:

$$G = p_a G_{ref} \left(\frac{p}{p_a}\right)^{Gexp} \quad (2)$$

Here, G_{ref} is the dimensionless stiffness factor, p_a denotes the atmospheric pressure, and G_{exp} serves as the exponent characterizing stress-dependency. The plastic hardening parameter H_{pl} is constant and independent of the initial state parameter ψ_0. Additionally, the NorSand model incorporates the volumetric coupling coefficient (N), the critical state friction angle (φ_{cs}), the Poisson's ratio (ν) and the parameter χ, which relates - under triaxial reference conditions - the maximum dilatancy to the state parameter.

The implementation of this model in the MPM code incorporates explicit Runge–Kutta time integration, along with automatic substepping and error control, as outlined by Sloan et al. (2001).

Figure 1 depicts the numerical CPT model, with a perfectly rigid cone penetrating an elasto-plastic soil. The cone radius (r_c) is 17,85 mm. The radius of the chamber is 362 mm, which corresponds to a cone-to-diameter ratio of about 20.

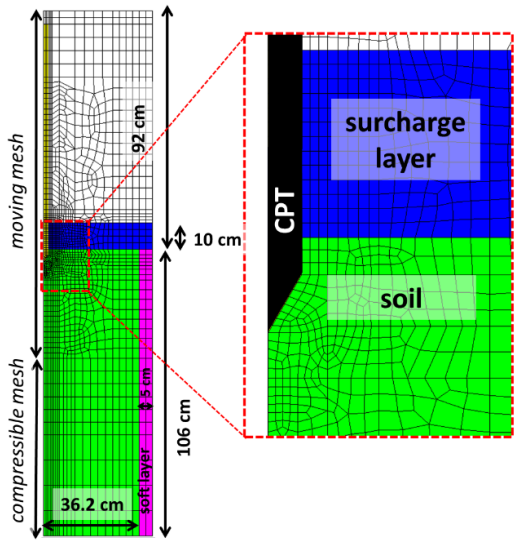

Figure 1: Numerical CPT model: geometry and background mesh for MPM calculations.

In all CPT simulation scenarios, the stress state was initialized with a soil pressure ratio K_0 set to 1, and the stress was kept constant on both top and radial boundary of the model. To do so, two layers of elastic material were introduced, named "surcharge layer" and "soft layer" respectively. The surcharge layer applies a vertical stress of 100 kPa at the top of the soil domain, while ensuring a perfectly smooth contact between the layer and the rigid cone. The lateral soft layer is fixed along its outer edge and it is very soft with a Young's modulus of 1 kPa. In all simulations, the soil was considered fully saturated, but no excess pore pressure was allowed during penetration, resulting in drained conditions.

2.2. Parametric study and dataset generation

In total, 125 MPM CPT simulations have been conducted using randomly generated parameters from the NorSand constitutive model, employing the hypercube approach. The parameter list is summarized in Table 1, where some parameters are kept constant while others are varied, with their intervals specified in brackets. A total of 6 NorSand parameters ($\lambda_e, G_{ref,0.5}, G_{exp}, \varphi_{cs}, H_{pl}, \chi$), the friction ratio ($R_c$), and the initial condition (ψ_0) were randomly varied for this study. The friction ratio is defined as the ratio between the tangent of the contact friction angle ($\tan(\varphi_c)$) and $\tan(\varphi_{cs})$.

It is worth mentioning that the intercept Γ_1 of the critical state line is set to a constant value, as its variation does not impact the results. Additionally, the value of the parameter N is also kept constant, as it does not have a significant contribution to the cone resistance, as pointed out by Yost et al. (2023).

Table 1: Range of values used for generating data for the NorSand model parameters and the contact friction ratio R_c

Parameter	**Values**
Γ_1	0.8
λ_e	[0.02 – 0.06]
$G_{ref,0.5}$	[50 – 500]
G_{exp}	[0.5 – 1.0]
ν	0.2
φ_{cs}	[30 – 36.0]
N	0.25
χ	[2.0 – 5.0]
H_{pl}	[25 – 400]
ψ_0	[-0.1 – 0.1]
R_c	[0.33 – 0.66]

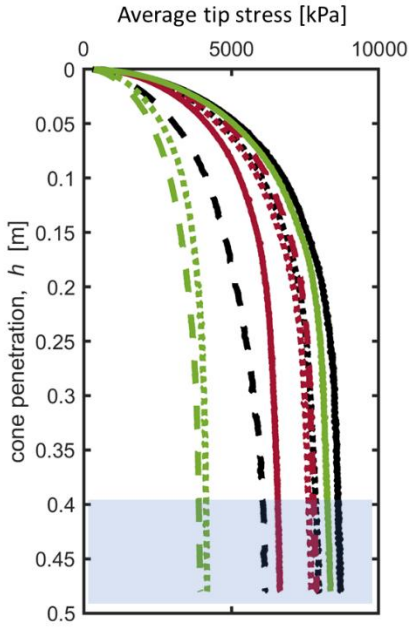

Figure 2: example of 10 CPT MPM simulations with random realization of the input parameters. The shaded area indicates where the q_c value is determined.

G_{exp} was varied randomly between 0.5 and 1.0, while $G_{ref,0.5}$ was varied randomly between 50 and 500. Here, $G_{ref,0.5}$ is the value of G_{ref} when G_{exp} = 0.5. The

conversion of $G_{ref,0.5}$ to the standard NorSand parameter G_{ref} was performed with the following equation:

$$G_{ref} = G_{ref,0.5}\left(\frac{p_{ref}}{p_a}\right)^{0.5-G_{exp}} \quad (3)$$

This equation ensures that G_{exp} determines the shape of the stress-dependent stiffness function, while the randomly assigned value $G_{ref,0.5}$ determines the value of the stiffness at p_{ref}. If p_{ref} is set equal to p_a, then the value of G_{ref} is identical to $G_{ref,0.5}$. It is worth noticing that, for $p_{ref} = p_a$, the elastic stiffness can result to extremely large values at high stresses when the exponent G_{exp} tends to 1.0. Given the large stresses induced during cone penetration test, in this study, the value of p_{ref} is set to 500 kPa to ensure that elastic stiffness does not reach unrealistic magnitudes.

Figure 2 presents the results of 10 CPT MPM analyses, illustrating the evolution of the average tip stress as a function of cone penetration. The input parameter set for each simulation is a random realization within the ranges specified in Table 1. In all cases, the cone resistance profile tends to plateau after a penetration of approximately 35 cm. Therefore, the average value of the tip stress reached after 40 cm of penetration was chosen as the q_c value.

All 125 q_c values are illustrated in ***Figure 3*** as function of the initial state parameter ψ_0.

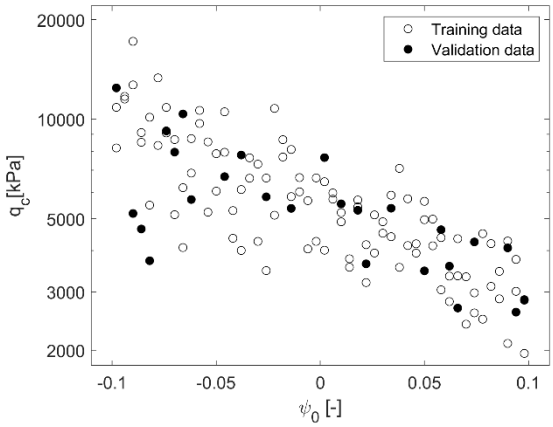

Figure 3: log-linear plot of the normalised cone resistance q_c/p_a against initial state parameter ψ_0.

3. Predictive equation for q_c

The dataset is used here to calibrate a predictive equation for the cone resistance q_c. The variables are independent; therefore, the proposed equation is written as follows:

$$ln(\frac{q_c}{p_a}) = ln(K) - (\psi_0 - 1)m + \varepsilon \quad (4)$$

Here, q_c is the cone resistance, $ln(K)$ and m are the intercept (at the ideal value of ψ_0 equal to 1) and the slope, respectively. Specifically, $ln(K) = \sum_{i=1}^{n} \alpha_i\, ln(C_i)$ and $m = \sum_{i=1}^{n} \alpha_{n+i}\, ln(C_i)$. The value of n denotes the number of dimensionless variables, which are 7 in this study, plus a constant (set as $ln(C_8)$). These variables are listed as follows:

$$ln(C_1) = ln\left(\frac{\tan(\varphi_c)}{\tan(\varphi_{cs})}\right) = ln(R_c) \quad (5)$$
$$ln(C_2) = ln(G_{ref,0.5}) \quad (6)$$
$$ln(C_3) = ln(G_{exp}) \quad (7)$$
$$ln(C_4) = ln\left(\frac{\lambda_e}{0.01}\right) \quad (8)$$
$$ln(C_5) = ln\left(\frac{6\sin(\varphi_{cs})}{3-\sin(\varphi_{cs})}\right) = ln(M_{cs}) \quad (9)$$
$$ln(C_6) = ln(H_{pl}) \quad (10)$$
$$ln(C_7) = ln(\chi) \quad (11)$$
$$ln(C_8) = ln(100) \quad (12)$$

The value of φ_c is the friction angle adopted in the simulation to describe the strength at the contact between the penetrometer and the soil. The coefficients α_i and α_{n+i} are determined via linear regression.

The database depicted in ***Figure 3*** is divided into two groups: the *training set*, represented by empty dots, which comprises 80% of the data, and the *validation set*, represented by full dots, which constitutes the remaining 20% of the dataset. The training set is utilized to determine the regression coefficients, while the validation set is employed to confirm the accuracy of the predictive equation.

From the training dataset the independent variables $X_i = \ln(C_i)$ (including ψ_0) are collected, together with the dependent variables $Y_j = ln(\frac{q_c}{p_a})$. For a single simulation, the value of the dependent variable is defined as Y_j, which corresponds to the data in the training dataset, and the estimate of the dependent variable is $\hat{Y}_j$. Eq. (4) can be written as follows:

$$\hat{Y}_j = \sum_{i=1}^{n} \alpha_i X_i - (\psi_0 - 1)\sum_{i=1}^{n} \alpha_{n+i} X_i \quad (13)$$

This expression can be further simplified into a compact form:

$$\hat{Y}_j = \boldsymbol{A}_j \boldsymbol{\alpha} \quad (14)$$

where $\boldsymbol{A}_j = [\boldsymbol{X}^T \quad -(\psi_0 - 1)\boldsymbol{X}^T]$. Here, $\boldsymbol{X}$ is a vector of size n listing all X_i, and $\boldsymbol{\alpha}$ is the coefficient vector with size $2n$, which lists all coefficients α_i and α_{n+i}.

The compact form that includes all independent variables is:

$$\hat{\boldsymbol{Y}} = \boldsymbol{A}\boldsymbol{\alpha} \quad (15)$$

The coefficient vector $\boldsymbol{\alpha}$ is finally determined as follows:

$$\boldsymbol{\alpha} = (\boldsymbol{A}^T\boldsymbol{A})^{-1}\boldsymbol{A}^T\boldsymbol{Y} \quad (16)$$

Eq. (4) is rewritten to explicitly compute the intercept at the ideal value of ψ_0 equal to 0 (instead of 1), as follows:

$$ln(\frac{q_c}{p_a}) = ln(K^*) - \psi_0\, m + \varepsilon \quad (17)$$

where $ln(K^*) = ln(K) + m$. The terms $ln(K^*)$ and m, with the coefficients determined by Eq. (16), are written as follows:

$$ln(K^*) = 0.25\, ln(R_c) + 0.26\, ln(G_{ref,0.5}) - 0.16\, ln(G_{exp}) - 0.23\, ln\left(\frac{\lambda_{CS}}{0.01}\right) +$$

$$2.00\,ln(M_{CS}) - 0.18\,ln(H_{pl}) - \\ -0.02\,ln(\chi) + 1.52 \quad (18)$$

$$m = -0.23\,ln(R_c) + 1.39\,ln(G_{ref,0.5}) - \\ 1.42\,ln(G_{exp}) - 0.06\,ln\left(\frac{\lambda_{CS}}{0.01}\right) + \\ 3.62\,ln(M_{CS}) + 0.33\,ln(H_{pl}) + \\ 4.10\,ln(\chi) - 9.76 \quad (19)$$

The random error term ε represents the difference between the observed values of the dependent variable and the values predicted by the regression equation. The random error term for each observation is written as follows:

$$\varepsilon_j = Y_j - \hat{Y}_j \quad (20)$$

It was found that the distribution of ε can be well approximated by a normal distribution, with a mean value of 0 and a standard deviation σ_ε of approximately 0.056.

The relative importance of each variable X_i is computed separately for $ln(K^*)$ and the slope m, and labeled β_i and β_{n+i}, respectively:

$$\beta_i = \frac{\alpha_i \sigma_{X_i}}{\sigma_{ln(K^*)}} \quad (21)$$

$$\beta_{n+i} = \frac{\alpha_{n+i} \sigma_{X_i}}{\sigma_m} \quad (22)$$

where $\sigma_{ln(K^*)}$ and σ_m are the standard deviation of the terms $ln(K^*)$ and m in Eq. (4), and σ_{X_i} is the standard deviations of the terms X_i. The importance of a parameter is high when the value of $|\beta_i|$ or $|\beta_{n+i}|$ tends to unity, whereas the parameter becomes less important when β is close to zero.

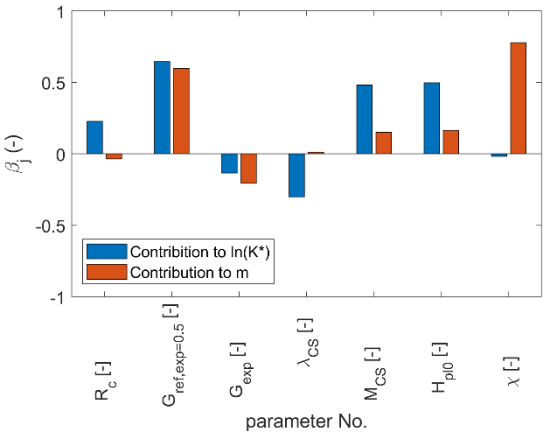

Figure 4: Relative importance of each variable with respect to ln(K*) and m.

Figure 4 shows that some variables X_i have a large relative influence on the outputs of the predictive equation, while others have a negligible contribution. Therefore, to consider only the most contributing variables in the predictive equation, some variables X_i were excluded from either $ln(K^*)$ or m. Since the contribution of these variables is not important, the overall standard deviation σ_ε remained practically unchanged (0.058).

The reduced terms $ln(K^*)$ and m of Eq. (17) are written as follows:

$$ln(K^*) = 0.25\,ln(R_c) + 0.26\,ln(G_{ref,0.5}) - \\ 0.17\,ln(G_{exp}) - 0.23\,ln\left(\frac{\lambda_{CS}}{0.01}\right) + \\ 2.03\,ln(M_{CS}) + 0.18\,ln(H_{pl}) + 1.54 \quad (23)$$

$$m = 1.34\,ln(G_{ref,0.5}) - 1.09\,ln(G_{exp}) + \\ 3.93\,ln(\chi) - 6.18 \quad (24)$$

Rewriting Eq. (23) and Eq. (24) with Eq. (3), provides the regression in standard NorSand input parameters:

$$ln(K^*) = 0.25\ln(R_c) + 0.26\ln(G_{ref}) - \\ 0.17\ln(G_{exp}) + 0.42(G_{exp} - 0.5) - \\ 0.23\ln\left(\frac{\lambda_{CS}}{0.01}\right) + 2.03\ln(M_{CS}) - \\ 0.18\ln(H_{pl}) + 1.54 \quad (25)$$

$$m = 1.34\ln(G_{ref}) - 1.09\ln(G_{exp}) + \\ 2.16(G_{exp} - 0.5) + 3.93\ln(\chi) - 6.18 \quad (26)$$

The comparison between *training data* and the corresponding values provided by Eq. (17), (25) and (26) is illustrated in ***Figure 5***.

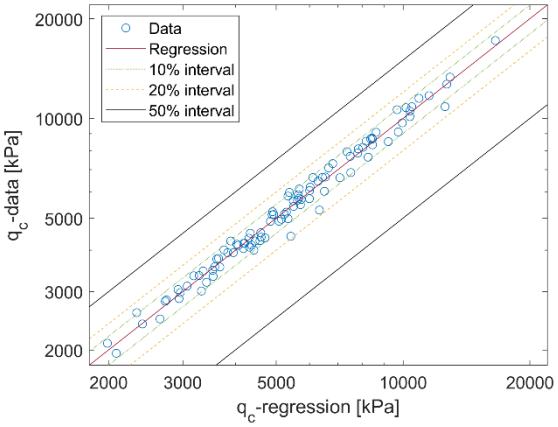

Figure 5: comparison between training data and the corresponding values using Eq. (17).

The *validation data* has been used to assess the accuracy of the predictive equation. The comparison is illustrated in ***Figure 6***. The data are closely aligned along the diagonal line, with deviation generally lower than 20%. It is worth noticing that the standard deviation σ_ε of the errors is approximately 0.065, which is slightly higher compared to the one obtained from the training data. This confirms the accurate performance of the predictive equation.

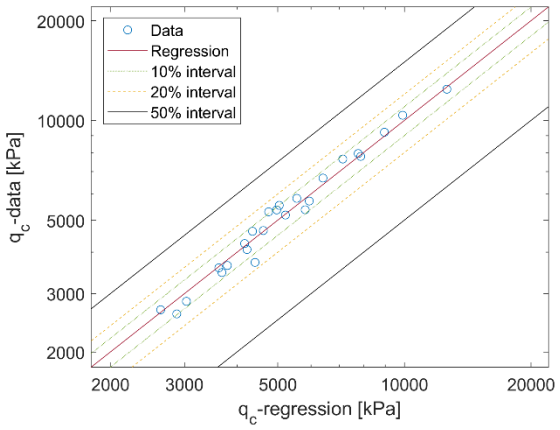

Figure 6: comparison between validation data and the corresponding values using Eq. (17).

4. Conclusions

This paper adopts the MPM framework proposed by Martinelli and Pisano (2022) and the framework of Martinelli and Galavi (2022) to simulate CPT chamber test data of coarse-grained deposits. Through extensive CPT MPM simulations based on the critical state NorSand model, a predictive equation for cone resistance is developed, accounting for the state parameter of the soil and the parameters of the constitutive NorSand model. The form of the predictive equation, easy to implement, enable practitioners to relate - for a specific soil - the cone resistance with the corresponding state parameter ψ. The predictive equation can be used for soils for which the $\lambda_e, G_{ref,0.5}, G_{exp}, \varphi_{cs}, H_0$ fall within the ranges of the dataset. Difference may be expected for different initial stress conditions. In future work, the predictive equation will be validated on experimental data, and expended to a wider dataset, which will also include the effect of initial stress conditions.

Acknowledgements

All the MPM simulations were performed using a specific version of Anura3D, developed in-house by Deltares. The authors thank Antonis Mavritsakis from Deltares, who set up the script for hypercube sampling and configured the tool for automatic CPT runs.

References

Al Kafaj, K.I., 2013. Formulation of a Dynamic Material Point Method (MPM) for Geomechanical Problems. *PhD thesis. Univ. of Stuttgart, Germany*.

Ayala, J., Fourie A, Reid D, (2022) Improved cone penetration test predictions of the state parameter of loose mine tailings. *Can. Geotech. J. 59: 1969–1980 (2022)* dx.doi.org/10.1139/cgj-2021-0460

Been, K. & Jefferies, M. G. (1985). A state parameter for sands. *Géotechnique 35, No. 2, 99–112*, https://doi.org/10.1680/geot.1985.35.2.99.

Ceccato, F., Beuth, L., Simonini, P., 2016a. Analysis of Piezocone Penetration under Different Drainage Conditions with the Two-Phase Material Point Method. J. Geotech. Geoenviron. Eng. 142 (12), 04016066. https://doi.org/10.1061/(asce)gt.1943-5606.0001550 .

Ceccato, F., Beuth, L., Vermeer, P.A., Simonini, P., 2016b. Two-phase Material Point Method applied to the study of cone penetration. Comput. Geotech. 80, 440–452. https://doi.org/10.1016/ j.compgeo.2016.03.003 .

Jefferies, M. & Been, K. (2016). *Soil liquefaction: a critical state approach*, 2nd edn. Boca Raton, FL, USA, CRC Press.

Jefferies,M. (1993). Norsand: a simple critical state model for sand. *Géotechnique 43, No. 1, 91–103*, https://doi.org/10.1680/ geot.1993.43.1.91.

Martinelli M, Pisano F (2022) Relating Cone Penetration Resistance to sand state using the material point method, *Geotechnics Letters 12, 1-8, 2022*

Martinelli, M., Galavi, V., 2021. Investigation of the Material Point Method in the simulation of Cone Penetration Tests in dry sand. *Comput. Geotech. 130, 103923*. https://doi.org/10.1016/ j.compgeo.2020.103923.

Martinelli, M., Galavi, V., 2022. An explicit coupled MPM formulation to simulate penetration problems in soils using quadrilateral elements. *Comput. Geotech. 145,104697*. https://doi.org/10.1016 /j.compgeo.2022.104697.

Sloan, S. W., Abbo, A. J. & Sheng, D. (2001). Refined explicit integration of elastoplastic models with automatic error control. Engng Comput. (Swansea) 18, No.1/2, pp. 121–194, https://doi.org/10.1108/02644400110365842.

Yost KM, Mario Martinelli, Alba Yerro, Russell A. Green, Dirk A. de Lange. Addressing complexities in MPM modeling of calibration chamber cone penetrometer tests in homogenous and highly interlayered soils. *Computers and Geotechnics 158 (2023) 105378*